euspen's 24th International Conference & Exhibition, Dublin, IE, June 2024
www.euspen.eu

Recycling of erosion sludge particles for laser beam direct energy deposition

Oliver Voigt[1], Moritz Lamottke[2,*], Marco Wendler[3], Henning Zeidler[2], Urs Peuker[1]

[1]*Institute of Mechanical Process Engineering and Mineral Processing, Technische Universität Bergakademie Freiberg, Agricolastr. 1, 09599 Freiberg, Germany*
[2] Institute for Machine Elements, Engineering Design and Manufacturing, Technische Universität Bergakademie Freiberg, Agricolastr. 1, 09599 Freiberg, Germany
[3]Institute of Iron and Steel Technology, Technische Universität Bergakademie Freiberg, Leipziger Straße 34, 09599 Freiberg, Germany

*correspondence *: moritz.lamottke@imkf.tu-freiberg.de & oliver.voigt@mvtat.tu-freiberg.de*

Abstract
Waste sludges from electro discharge machining were collected from the bottom of the machining basin. These contain eroded metallic particles, which are suitable for processes in additive manufacturing regarding their size ranges, shape and bulk powder properties. After cleaning and classifying, these particles with high carbon contents were used to clad beads and layers via laser beam direct energy deposition, where defect free structeres could be obtained. These were analyzed regarding their dilution ratio, microstructure and hardness. Microstructures featuring pearlite, austenite, martensite and cementite due to mixtures of high carbon particles and low carbon substrate were observed. The beads and layers show overall high hardness of 700 HV10 to 960 HV10.

Keywords: Additive Manufacturing, Laser Beam Direct Energy Deposition, Recycled Particles, Microstructure, Hardness, Electro Discharge Machining

1. Introduction

The production of metal powders for additive manufacturing (AM) by gas atomization is an energy- and cost-intensive process. Therefore, it is indispensable to focus on alternatives for providing powders. One possibility seems to be waste sludge from electro discharge machining (EDM), which is accumulating at the bottom in machining basins and can be collected. In die-sink EDM, the material gets molten and vaporized by conversion of electrical into thermal energy. Removed material solidifies in the surrounding dielectric fluid (oil). The resulting particles achieve key size, shape and flowability parameters similar to AM powders [1].

A common AM-technique is laser beam directed energy deposition of metal powders (DED-LB/M). This process uses a laser to weld gas guided powder streams layer by layer to a substrate material. Narrow distributed and spherical particles with good flowability are necessary for successfully deposited beads [2]. Influenced by several operational settings and materials, different microstructures and mechanical properties can be achieved. In this study, recycled EDM particles are processed via DED-LB/M to show a use case for recycling EDM sludges. Investigations regarding microstructure and hardness of deposited structures are presented.

2. Materials and Methods

2.1. EDM Particles

Waste sludge was collected from a mold production company, where commercial H11 alloy was EDM-machined with a graphite electrode in a synthetic hydrocarbon-based dielectric with unkown settings. The oily phase was dissolved in acetone and metallic particles dried overnight. Fractions were obtaind by sieving. Particles of the size range 20 µm to 63 µm were used for DED-LB/M. Particle sizes and shapes were investigated via laser diffraction and dynamic image analysis. Chemical compostion was measured via ICP-OES and C-S-O analyzer. Hausner ratio was determined by measuring bulk and tap densities.

2.2. Specimen Prodution in DED-LB/M

Deposited beads (B1-B3) and layers (L1+L2) were created of pure EDM particles in a DED-LB/M device LV Midi (Laservorm GmbH, Germany) with a fibre laser source of maximum 1.5 kW. Used parameters are a laser power P of 1.4 kW, laser scan speeds v between 5 mm/s (B1+B2) and 50 mm/s (B3, L1, L2), powder flow rates of 7.91 g/min (B1+B2) or 15.87 g/min (B3, L1+L2), spot size of 0.9 mm, defocus between 15 mm and 30 mm and gas purge flows of 8 l/min (particles) and 16 l/min (inside). A mild construction steel was used as substrate. The dilution ratio α (Eq. 1), whereas d is the height of the deposited bead and h the depth of the molten pool, and linear heat input H (Eq. 2) were calculated for evaluating the deposition result. Values were obtained Fiji ImageJ software.

$$\alpha = \frac{d}{h+d} \times 100 \qquad (1)$$

$$H = \frac{P}{v} \qquad (2)$$

2.3. Microstructure Analysis and Hardness Measurement

The deposited beads, layers and substrate microstructure was examined via light microscopy. Samples were embedded in Polyfast matrix and cut in half. Afterwards, the surfaces were ground with SiC paper, polished with diamond suspension and colloidal silica and etched in Nital. Hardness values of minimum five locations per bead and layer were measured according to Vickers method HV10 with 10 kP for 10 s on the surfaces used for microstructure analysis. A device KB 30 S was used with settings with KB Hardwin XL software.

3. Results and Discussion

3.1. Particle Properties

After sieving, the recycled EDM particles show a narrow particle size distrubtion (table 1). The size parameters are compared to commercial H11 particles. The circularity is on a similar high level ensuring a good flowability, which is confirmed in the determined Hausner ratios. These do not show a

significant difference, whereas the tap and bulk densities are different by approx. 5 %.

Table 1: Characteristic particle properties of H11 reference and eroded particles for DED-LB/M

Property	H11 reference	Eroded particles
$x_{10,3}$ in µm	19.4	22.8
$x_{50,3}$ in µm	30.1	39.5
$x_{90,3}$ in µm	61.7	60.6
Circularity	0.93	0.92
Hausner ratio	1.05	1.06

The chemical composition of EDM particles equals the H11 alloy composition except the high carbon content of approx. 4.9 wt.%. Due to high temperature gradients, when the molten material solidifies in the dielectric, a high temperature carbon uptake takes place and C is entrapped in the Fe lattice caused by a pyrolysis of the dielectric [3]. Additional information about these EDM particles regarding morphology, XRD and phase analysis as well as their microstructure can be found in [4].

3.2. Appearence of Deposited Structures

Beads and single layers were successfully deposited with nearly no thermal or residual stress cracks despite the high carbon content. During the DED-LB/M process, a high evaporation rate was observed. Deposited structures appear smoothly shaped, and the melt pool and heat affected zone depth rule out effects of keyholing or lack of fusion. Just a few gas entrapments and barely any non-metallic inclusions are seen. Fig. 1 shows calculated dilution ratios against linear heat input with an exemplary bead in the top containing two smaller pores. Common dilution ratios are in the range of 10 % to 30 % [5], which is fulfilled by nearly all samples. Pre-heating the substrate (L2) leads to better and even crack-free results.

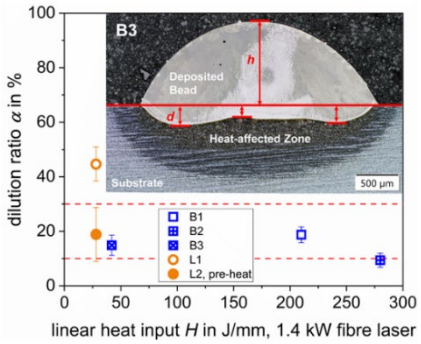

Figure 1: Dilution ratio against linear heat input of 3 deposited beads and 2 layers with micrograph of whole bead

3.3. Microstructure of Structures

Fig. 2 shows different microstructural areas of substrate and beads. Former one exhibits a fine-grained high-ferritic and low-pearlitic microstructure with a low carbon content. B1 features a fine-lamellar pearlitic microstructure with whiteish austenite dendrites corresponding with local hardness values. The composition of this region is clearly shifting to the eutectoid steel region, as no cementite is present, resulting from a mixture of high-C particles and low C-substrate as well as carbon evaporation. In B2 acicular primary cementite and pearlite are observed, as cementite can develop in the top region of the bead due to non-mixing of components as in the boundary region. Latter one is shown in B3 containing cementite in upper regions and known fine-lamellar pearlitic and dendritic austenite. In the heat-affected zone a martensitic structure is present as result of a mixture of substrate and eroded particle, which is solidifying austentic with high cooling gradients leading to a tetragonal distortion.

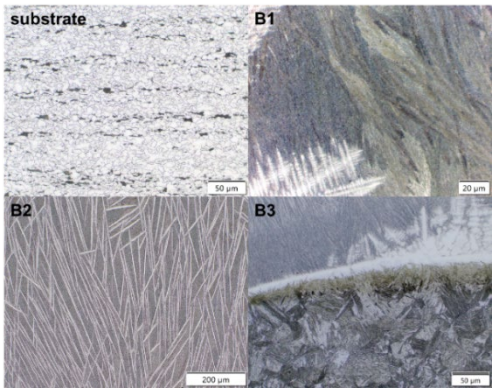

Figure 2: Micrographs of the substrate material and deposited beads B1-B3 at different phase regions

Fig. 3 shows the micrographs of deposited layers. In L1, one of several elongated residual stress cracks, related to high C, is observable surrounded by primary cementite needles. Moreover, some smaller areas are appearing as non-metallic inclusions. In general, the fine-lamellar pearlitic and dendritic austenitic microstructure is present again. For L2, a nucleation origin at the right edge with directed crystallization to the centre, possibly caused by a particle, can be assumed.

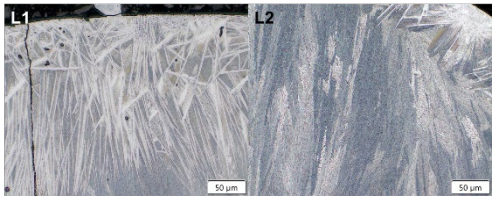

Figure 3: Microstructural image of deposited layer L1+L2

3.4. Hardness of Deposited Structures

As it can be assumed by carbon content and developed microstructures, quite high hardness ranging from 700 HV10 to 960 HV10 (see Tab. 2) is observable. Due to cracks and defects, the value for L1 is significantly lower. B2 shows the highest value due to the presence of hard and wear-resistent cementite.

Table 2: HV10 hardness values 3 deposited beads and 2 layers

Sample	HV10
B1	**704** ± 102
B2	**961** ± 21
B3	**834** ± 171
L1	**516** ± 36
L2	**920** ± 54

4. Outlook

DED-LB/M process was successfully used to deposite beads and layers using recycled EDM particles. Microstructure as well as hardness were analyzed. Deposited structures exhibit microstructures containing pearlite, austenite, martensite and cementite and show overall high hardness values. Future works will focus on powder mixtures with pristine particles to further decrease the C-content and supress the occurrence of cracks as well as enhance the final properties.

References

[1] Voigt, O. and Peuker, U.A., *Metals*, 2022. **12**(9).
[2] Ahn, D.-G., *International Journal of Precision Engineering and Manufacturing-Green Technology*, 2021. **8**(2): p. 703-742.
[3] Berkowitz, A.E. and J.L. Walter, *Journal of Materials Reasearch*, 1987. **2**(2): p. 277-288.
[4] Voigt, O., Wendler, M., Siddique, A., Stöcker, H., Quitzke, C. and Peuker, U.A., *Metals and Materials International*, 2023.
[5] Dass, A. and A. Moridi, *Coatings*, 2019. **9**(7).